MURINE INTERLEUKIN 7 (IL-7) RECEPTOR

Characterization on an IL-7-dependent Cell Line

By LINDA S. PARK, DELLA J. FRIEND, ANN E. SCHMIERER, STEVEN K. DOWER, and ANTHONY E. NAMEN

From the Immunex Corporation, Seattle, Washington 98101

Significant progress has been made in recent years regarding the delineation of the role of soluble mediators in hematopoiesis. Colony-stimulating factors have now been described at a molecular level for most of the cells of the myeloid lineage (1), and an ever increasing number of mediators are now known to regulate lymphocytes (2), the major effector cells of the immune response. Much less is known about the molecular nature of the regulators that control development of lymphoid progenitors. Recently we described the isolation and cloning of IL-7 (3, 4). IL-7 was originally detected and isolated on the basis of its potent proliferative effects on B cell progenitors derived from long-term bone marrow cultures (3). Interestingly, IL-7 has now been shown to stimulate T cell progenitors (5–7) and is emerging as a major element in the development of both B and T lymphocytes. In addition, it is now clear that IL-7 can stimulate mature peripheral T cells (8, 9), and T cell clones (10); however, the complete repertoire of cells responsive to IL-7 is still under investigation.

In an effort to more clearly define the cells responsive to IL-7, we now describe the initial characterization of the murine IL-7 receptor and the cellular distribution of such receptors. We have developed a clonal cell line (IxN/2b) that is absolutely dependent upon IL-7 for growth and viability and have used this cell line to define the binding and structural characteristics of the murine IL-7 receptor. Additionally, we have investigated the distribution of IL-7 receptors on an extensive library of cell lines and primary tissues.

Materials and Methods

The IxN/2b Cell Line and Bioassay for IL-7. This cell line was obtained by IL-7-dependent limiting dilution cloning of the nonadherent cells from a long-term Whitlock-Witte bone marrow culture as previously described (3). These cells have now been in continuous culture for more than 24 mo and have retained a strict growth dependence upon exogenous IL-7. The cells were routinely passaged by dilution to 2×10^4 cells/ml every 3 d in Iscove's modified Dulbecco's Medium (IMDM)[1] containing 5% FCS, 5×10^{-5} M 2-ME, 2 mM L-glutamine, 50 μg/ml streptomycin, and 50 U/ml penicillin (assay medium) containing 2,000 U/ml of recombinant murine IL-7. IxN/2b is used as the indicator cell line for routine assessment

Address correspondence to Dr. Linda S. Park, Immunex Corp., 51 University Street, Seattle, Washington 98101.

[1] *Abbreviations used in this paper:* EGF, epidermal growth factor; IMDM, Iscove's modified Dulbecco's medium; PDGF, platelet-derived growth factor.

of IL-7 concentrations in sample solutions as opposed to using nonadherent cells from long-term Whitlock-Witte bone marrow cultures. IL-7 assays were performed essentially as described earlier (3). Briefly, IxN/2b cells were pelleted by centrifugation, washed twice, resuspended in assay medium, and added in 50-μl aliquots (1.2×10^5 cells/ml) to microtiter plates that contain varying concentrations of IL-7 or test samples. The cells were incubated for 48 h in a reduced oxygen atmosphere containing 7.5% CO_2 and 5% O_2 and pulsed during the final 4 h of incubation with 2 μCi/well of [^{3}H]TdR (60–80 Ci/mmol; New England Nuclear, Boston, MA). The cells were then harvested and the radioactivity was determined by standard liquid scintillation counting.

Cell Preparations. All cell lines were grown in RPMI-1640 (Gibco Laboratories, Grand Island, NY) containing 5–20% FCS and antibiotics, except IxN/2b which were maintained as described above. Abl1.1 cells were derived from murine BALB/c bone marrow using Abelson murine leukemia virus as detailed by Rosenberg and Baltimore (11). The resultant macroscopic colonies were plucked and expanded in liquid culture as needed. These cells exhibited a pre-B cell phenotype (surface μ-negative, cytoplasmic μ-positive).

Murine B cells (12) and murine bone marrow-derived macrophages (13) were prepared as previously described. Single cell suspensions were isolated from whole thymus, peripheral lymph node, and spleen following mechanical dissociation and centrifugation to remove cell debris. Spleen cell populations were also subjected to hypotonic lysis to remove contaminating red blood cells.

Cytokines and Hormones. Recombinant human IL-1α and β (14), murine granulocyte/macrophage (GM)-CSF (15), and murine IL-4 and human IL-2 (16) were produced and purified as previously described. Human G-CSF, CSF-1, IL-5, and TNF-α were constructed as fusion proteins containing an additional octapeptide at the NH_2 terminus, expressed in yeast, and purified as previously described (17, 18). Human IL-6 was cloned as described elsewhere (8), expressed in yeast, and partially purified by chromatography on S-Sepharose (Pharmacia Fine Chemicals, Piscataway, NJ). *Escherichia coli*-derived human TNF-β was obtained from R & D Systems Inc. (Minneapolis, MN). Human TGF-β was obtained from Collaborative Research (Bedford, MA). Murine epidermal growth factor (EGF) was obtained from Sigma Chemical Co. (St. Louis, MO), and human insulin was obtained from Calbiochem-Behring Corp. (La Jolla, CA).

Cell Surface Analysis. Expression of cell surface antigens was determined by labeling 5×10^5 cells with a primary antibody followed by labeling with fluorescein-conjugated goat anti-rat Ig or goat anti-mouse Ig (Tago, Inc., Burlingame, CA). The mAbs used were: anti-Thy-1, clone T24-31.7 (19); anti-Ly-1, clone 53.73 (20); anti-J11D (21); anti-IL-2R, 7D4, specific for murine p55 (22); PK136, specific for the NK1.1 Ag (23); anti-Pgp-1 (24); 14.8 (anti-Ly5/220) (25); BP1 (Dr. M. D. Cooper, University of Alabama, Birmingham, AL); anti-Mac-1 (26). Fluorescein-conjugated goat F(ab')$_2$ anti-murine IgM (μ chain specific) was purchased from Tago, Inc. Fluoresceinated anti-murine κ and λ were obtained from Fischer Biotech (Orangeburg, NY). Labeled cells were analyzed using an EPICS-C flow cytometer (Coulter Electronics, Hialeah, FL).

Recombinant IL-7 Purification and Radiolabeling. Murine IL-7 was purified from supernatants of COS-7 monkey kidney cells transfected with the murine IL-7 clone 1046B (4) as previously described (3). After purification, IL-7 concentrations were determined by amino acid analysis, and activity was measured in the IxN/2b proliferation assay. Purified IL-7 was radiolabeled using the enzymobead radioiodination reagent (Bio-Rad Laboratories, Richmond, CA) as previously described for murine recombinant GM-CSF (27). Radiolabeled stocks were stored at 4°C in RPMI-1640 containing 2% BSA, 20 mM Hepes buffer, and 0.2% sodium azide, pH 7.2 (binding medium). Bioactivity was determined in the IxN/2b assay on samples in which sodium azide had been deleted. The specific activities of radiolabeled preparations were based on determination of an initial protein concentration by amino acid analysis, with correction from control experiments to determine protein recovery after iodination, in which an aliquot of IL-7 was spiked with ^{125}I-IL-7 and put through the iodination protocol with omission of ^{125}I.

Binding Assays and Data Analysis. Binding assays were performed by a phthalate oil separation method (28) as previously described (27). Nonspecific binding was measured using ei-

ther a 500-fold or greater molar excess of unlabeled IL-7 or rabbit serum raised against murine IL-7 at a concentration that was shown in control experiments to equivalently inhibit ^{125}I-IL-7 binding. In either case unlabeled IL-7 or polyclonal serum was mixed with ^{125}I-IL-7 before addition of cells.

Association and dissociation kinetic experiments were conducted as previously described (27) and analyzed with functions that are single or sums of exponential terms as described elsewhere (29). Curvilinear equilibrium binding data were analyzed using an equation consisting of the sum of two simple Michaelis-Menten terms as previously described (18, 30). Inhibition data were analyzed with an equation for competitive inhibition between two ligands for two types of sites that consists of the sum of two simple terms as described elsewhere (18). Curve fitting was done using RS/1 (Bolt, Beranek and Newman, Boston, MA), a commercially available data processing package running on a Microvax II under the VMS operating system.

Affinity Crosslinking. IxN/2b cells (1.5×10^7) were incubated with ^{125}I-IL-7 (1×10^{-9} M) in the presence or absence of unlabeled IL-7 (1×10^{-6} M) for 2 h at 4°C. The cells were then washed twice in PBS at 4°C and bis-(sulfosuccinimidyl) suberate (BS^3) was added to a final concentration of 0.1 mg/ml. After 30 min at 25°C the cells were washed and resuspended in 150 μl of PBS/1% Triton containing 2 mM PMSF, 10 μM pepstatin A, 10 μM leupeptin, 2 mM *o*-phenanthroline, 2 mM EGTA, 1.25 mM benzamidine, 0.5 mM EDTA, 2 μg/ml soybean trypsin inhibitor, and 20 μg/ml E-64 for 5 min at 4°C, centrifuged at 12,000 *g* for 10 min, and the supernatants were retained.

SDS-PAGE. Samples were boiled for 3 min in sample buffer (0.06 M Tris-HCl, pH 6.8, 2% SDS, 10% glycerol) with or without 5% 2-ME and analyzed on 8% or 10–20% gradient gels by the procedure of Laemmli (31). Methyl ^{14}C-labeled molecular markers were purchased from Bethesda Research Laboratories (Gaithersburg, MD). After electrophoresis, gels were stained with Coomasie blue (0.25% in 25% isopropanol, 10% acetic acid), dried, and exposed to Kodak X-Omat AR film at −70°C.

Results

Cell Surface Analysis of IxN/2b. The IxN/2b cell line is absolutely dependent upon exogenous IL-7 for continued growth. To determine the cell surface phenotype of this line, IxN/2b cells were stained with a variety of mAbs and analyzed using an EPICS-C flow cytometer. Some of the results are depicted in Fig. 1. The cells expressed detectable levels of the lymphoid precursor antigens, Pgp-1, BP-1, and J11D.

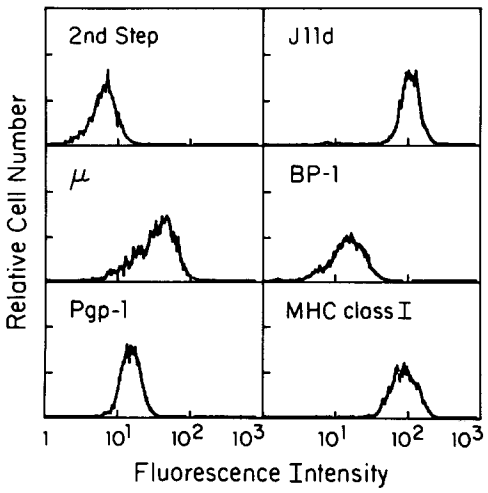

FIGURE 1. Cytofluorographic analysis of the B lineage cell line IxN/2b. The surface phenotype was assessed by immunofluorescence following incubation with rat or mouse mAbs as the primary antibodies and FITC-conjugated goat anti-mouse Ig or rat Ig, as needed, as the secondary reagent. The cells were incubated for 30 min at 4°C in the indicated primary antibody, washed 3× in PBS containing 1% BSA, and incubated another 30 min at 4°C with the secondary reagent. Following washing, the cells were analyzed using an EPICS-C flow cytometer.

The IxN/2b cell line is, however, B lineage committed, as it contained a rearranged μ heavy chain and a germline light chain (data not shown). The cells expressed high levels of class I MHC antigen but did not express detectable levels of class II molecules, consistent with an immature phenotype. Interestingly, the cells expressed surface μ in the absence of light chain rearrangement and expression. The cells were negative for cell surface expression of the lineage-specific markers: myeloid lineage (Mac-1), T cell lineage (Thy-1), B lineage (B220) and natural killer cells (NK1.1). Additionally, the cells did not express the Ly-1 marker, the IL-2 receptor (p55), or the Fc receptor. It would appear therefore that the IxN/2b cell line is an example of an early B cell progenitor that displays aberrant expression of μ chain in the absence of light chain expression. Given that this cell line was dependent upon IL-7, we hypothesized that it should express specific receptors for IL-7. Accordingly, we began our characterization of the IL-7 receptor using the IxN/2b cell line.

Radiolabeling of Murine IL-7. Recombinant murine IL-7 was purified to apparent homogeneity by previously described methods (3), and iodinated with the enzymobead radioiodination reagent. Fig. 2 A shows an autoradiograph of an iodinated murine IL-7 preparation that migrates as a broad band following SDS-polyacrylamide gel electrophoresis (average M_r of ~25,000). Radiolabeled preparations consistently displayed specific activities in the range of 2–4 $\times$ 10^{15} cpm/mmol (average of 2.8 $\pm$ 0.2 $\times$ 10^{15} from 15 separate iodinations). Murine IL-7 contains only one tyrosine residue which is very near the NH_2 terminus (amino acid 12), and judging from the average specific radioactivity obtained, it appears that this residue is being nearly quantitatively radiolabeled. In addition, when the biological activities of such preparations were measured in the IxN/2b proliferation assay they were found to retain 100% of their biological activity (Fig. 2 *B*). Given the presence of a single tyrosine residue as a target for labeling with ^{125}I, and the full retention of biological activity following radiolabeling, it is likely that the ^{125}I-labeled IL-7 preparations are relatively homogeneous. In addition, radiolabeled preparations were subjected to gel filtration chromatography on a Pharmacia FPLC system using a Superose 12 column (Pharmacia Fine Chemicals), and it was found that the radiolabeled protein migrated as a single major peak with an M_r of 20–30 $\times$ 10^3 (data not shown). No higher molecular weight aggregates were observed. An identical profile was obtained when

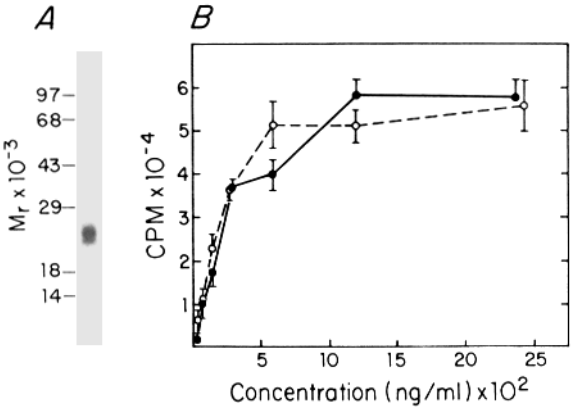

FIGURE 2. Characterization of ^{125}I-IL-7 by SDS-PAGE and proliferative response of IxN/2b cells. (*A*) ^{125}I-IL-7 (specific radioactivity, 2.8 $\times$ 10^{15} cpm/mmol) was boiled in sample buffer containing 2% SDS and 5% 2-ME and 10,000 cpm were applied to a linear 10–20% gradient gel. Electrophoresis and autoradiography were conducted as described under Materials and Methods. (*B*) IxN/2b cells were cultured in the presence of varying concentrations of IL-7 (○) or ^{125}I-IL-7 (●) and proliferative response was assayed as described under Materials and Methods.

^{125}I-IL-7 was preincubated with high concentrations of unlabeled IL-7 before chromatography, substantiating further that IL-7 does not appear to have a propensity towards self-association.

Kinetic and Equilibrium Binding Characteristics. Binding studies with radiolabeled IL-7 showed that it exhibited relatively rapid, specific, and saturable binding to IxN/2b cells at both 37° and 4°C. Fig. 3 illustrates IL-7 association kinetics, which shows that both at 4°C (Fig. 3 *A*) and 37°C (Fig. 3 *B*) the final equilibrium amount of ligand bound to cells and the approach to equilibrium are dependent upon the initial concentration of ^{125}I-IL-7 in the medium. The time required to reach equilibrium at 37°C is much shorter (<15 min) than the time required at 4°C (~2 h). The data depicted in Fig. 3, *A* and *B*, were analyzed both with an exponential function describing time-dependent binding to a single class of receptors, and with a function containing the sum of two exponential terms which describes time-dependent binding to two classes of receptor sites. Both models produced very similar fitted curves. The curves shown passing through the data in Fig. 3, *A* and *B*, were generated using a one-site model. Fig. 3 *C* shows plots of the pseudo-first-order associa-

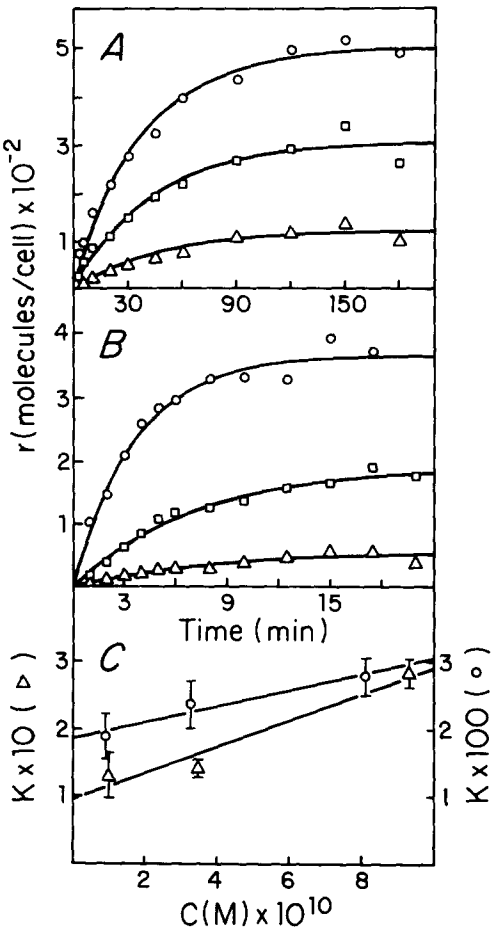

FIGURE 3. Association kinetics of ^{125}I-IL-7 with IxN/2b cells. IxN/2b cells (1.33×10^7 cells/ml) were incubated with 8.1×10^{-10} M (O), 3.3×10^{-10} M (□), or 9.0×10^{-11} M (Δ) ^{125}I-IL-7 at 4°C (*A*) or 9.3×10^{-10} M (O), 3.5×10^{-10} M (□) or 1.0×10^{-10} M (Δ) ^{125}I-IL-7 at 37°C (*B*). At the times indicated, aliquots were removed and assayed for binding as described under Materials and Methods. All data were corrected for nonspecific binding and the continuous curves passing through the data were calculated from the best-fit parameter values using a simple exponential term as described under Materials and Methods. Infinite time binding (molecules/cell) and pseudo first-order association rate constants (M^{-1} min^{-1}) calculated for each curve were, respectively, *A* (O) 496 ± 16 and 2.8 ± 0.3 $\times 10^{-2}$; (□) 302 ± 15 and 2.4 ± 0.4 $\times 10^{-2}$; (Δ) 123 ± 9 and 1.9 ± 0.3 $\times 10^{-2}$ and *B* (O) 367 ± 9 and 0.28 ± 0.02; (□) 194 ± 8 and 0.14 ± 0.01; (Δ) 55 ± 6 and 0.13 ± 0.03. (*C*) Pseudo first-order association rate constants calculated from the curves in *A* (O) and *B* (Δ) vs. the molar concentration [C] of ^{125}I-IL-7 initially present in the medium. The line passing through the data was generated by linear least squares analysis. The pseudo first-order association rate constants (k) are related to the association rate constant k_1 (second-order) and the dissociation rate constant k_{-1} (first-order) by the equation $k = k_1[C] + k_{-1}$ where the forward and reverse rate constants of ^{125}I-IL-7 can be determined, respectively, from the slope and ordinate intercept of the fitted lines.

tion rate constants determined from the curves in Fig. 3, *A* and *B*, relative to the initial concentration of ^{125}I-IL-7 in the medium. The forward and reverse rate constant of ^{125}I-IL-7 can be determined respectively from the slope and ordinate intercept of the fitted lines. From the average of two separate experiments at each temperature, the values obtained for 37 and 4°C were, respectively, $1.7 \pm 0.2 \times 10^8$ and $1.4 \pm 0.2 \times 10^7$ M^{-1} min^{-1} for the forward rate constants and 0.11 ± 0.01 and $1.6 \pm 0.3 \times 10^{-2}$ min^{-1} for the reverse rate constants. These data show that both the association and dissociation rates at 37°C are ~10-fold higher than those at 4°C. Due to this 10-fold difference in both rate constants, the binding affinity of radiolabeled IL-7, estimated from the ratio of these two constants, would nonetheless be predicted to be similar at 4°C and 37°C (8.7×10^8 M^{-1} and 1.5×10^9 M^{-1}, respectively).

Fig. 4 illustrates typical equilibrium binding data for ^{125}I-IL-7 to IxN/2b cells at both 4°C (Fig. 4 *A*) and 37°C (Fig. 4 *B*). Scatchard analysis of the data yielded a curvilinear plot at both temperatures. The curves passing through the points have been fit with an equation consisting of the sum of two Michaelis-Menten terms (30).

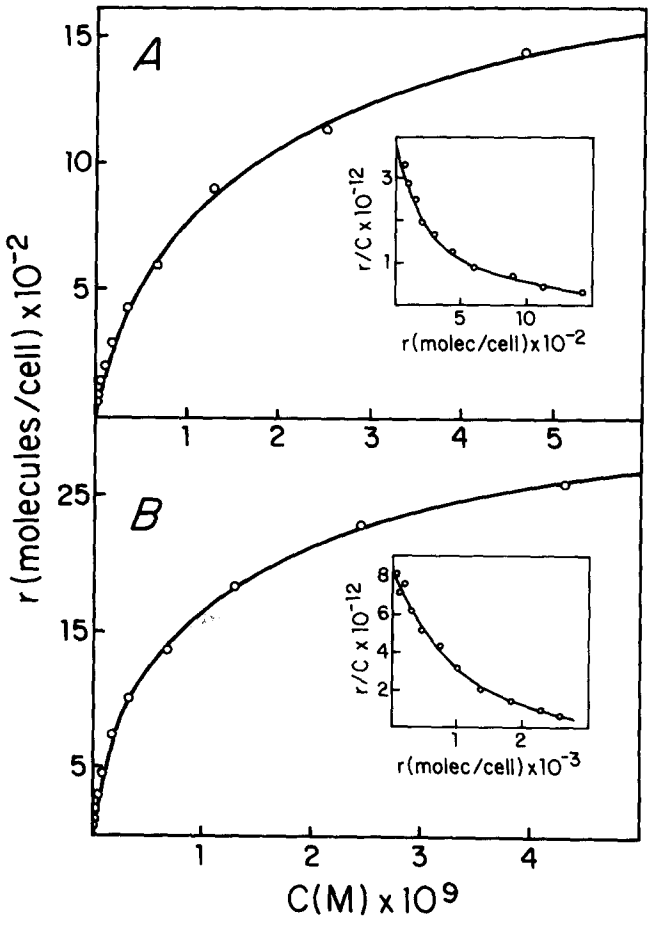

FIGURE 4. Equilibrium binding of ^{125}I-IL-7 to IxN/2b cells. Various concentrations of ^{125}I-IL-7 were incubated with IxN/2b cells (3.3×10^7 cells/ml) for 2 h at 4°C (*A*) or with IxN/2b cells (1.33×10^7 cells/ml) for 30 min at 37°C (*B*). Binding was assayed as described under Materials and Methods and all data were corrected for nonspecific binding. The insets show Scatchard representations of specific binding replotted from *A* and *B*. Curve fitting was done as described in Materials and Methods.

From the average of nine binding experiments at 4°C, IL-7 binding to IxN/2b cells displayed a high affinity component with an apparent K_a of 1.2 ± 0.1 × 10^{10} M^{-1} and 325 ± 55 specific binding sites per cell and a low affinity component with an apparent K_a of 3.9 ± 0.5 × 10^8 M^{-1} with 1,983 ± 226 specific binding sites per cell. Equilibrium binding parameters measured at 37°C were very similar. From the average of 11 binding experiments at 37°C a high affinity component with an apparent K_a of 8.8 ± 0.6 × 10^9 M^{-1} and 543 ± 68 specific binding sites per cell and a low affinity component with an apparent K_a of 4.8 ± 0.6 × 10^8 M^{-1} with 1,963 ± 148 specific binding sites per cell were obtained.

Direct measurement of the binding affinity of unlabeled IL-7 by inhibition of binding of ^{125}I-IL-7 to IxN/2b cells at 37°C is shown in Fig. 5. We found the data could not be adequately analyzed using a single-site competitive inhibition equation. However, when the data were fit with an equation for competitive inhibition between two ligands for two types of sites, the curve shown in Fig. 5 was obtained, which exhibits an excellent fit to the experimental points. From an average of three inhibition experiments we found the high affinity component displayed a K_I value of 2.7 ± 0.5 × 10^{10} M^{-1} with a maximal level of inhibition of 37.5 ± 2.9% and the low affinity component a K_I value of 4.1 ± 1.5 × 10^8 M^{-1} with a maximal level of inhibition of 60.9 ± 2.3. These values are very similar to those obtained by direct binding with ^{125}I-IL-7 and substantiate the existence of two classes of binding sites for IL-7 on IxN/2b cells.

There are several possible reasons for the appearance of curvilinear Scatchard plots, including the presence of two independent binding sites with different affinities, the presence of negative cooperative interactions, or both. As first described in the model of Demeyts et al. (32), a diagnostic test for the presence of negative cooperativity is an accelerated dissociation rate of radiolabeled ligand when measured in the presence of an excess of unlabeled ligand. Fig. 6 shows the dissociation of ^{125}I-IL-7 from IxN/2b cells at 4°C (Fig. 6 *A*) and 37°C (Fig. 6 *B*). At both temperatures, dissociation was measured in medium alone, where a fraction of the receptors are occupied, and in the presence of 8 × 10^{-8} M unlabeled IL-7, where most of the receptors are occupied. Several features of the data can be observed. First, the dissociation rate at 4°C with or without IL-7 in the media was very slow. In addition, the data could

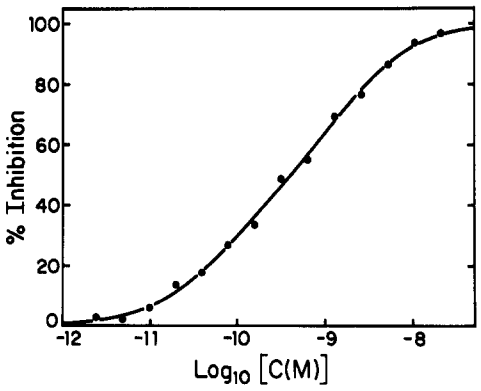

FIGURE 5. Inhibition of ^{125}I-IL-7 binding to IxN/2b cells by unlabeled IL-7. IxN/2b cells (2 × 10^7 cells/ml) were incubated with ^{125}I-IL-7 (3.7 × 10^{-11} M) and varying concentrations of unlabeled IL-7. Incubation was for 30 min at 37°C and binding was assayed as described under Materials and Methods. The continuous curve passing through the data was calculated from a two-site competitive inhibition equation using K_a values for ^{125}I-IL-7 of 9.2 × 10^9 M^{-1} (high affinity) and 4.2 × 10^8 M^{-1} (low affinity). All data were corrected for nonspecific binding measured in the presence of 5 × 10^{-8} unlabeled IL-7.

be suitably analyzed with an exponential function that describes a simple first-order process to produce the curves passing through the data in Fig. 6 *A*. In contrast, at 37°C a distinct biphasic kinetic pattern was observed that consisted of a very rapid initial dissociation rate followed by an extremely slow component that appears essentially irreversible. In the presence of unlabeled IL-7 in the media, the initial dissociation rates at both 37 and 4°C were significantly enhanced (see legend to Fig. 6). In addition, at 37°C the irreversible component of dissociation was eliminated, with the amount of specifically bound ^{125}I-IL-7 dropping to background levels (nonspecific binding) within 30 min. These data indicate that the rate of dissociation of IL-7 from IxN/2b cells is sensitive to receptor occupancy, and suggest that IL-7 receptors on IxN/2b cells exhibit negative cooperative behavior. Such behavior would result from decreasing affinity of IL-7 binding with increasing receptor occupancy and would predict that curvilinear binding curves might be obtained from equilibrium binding experiments.

The reason for the essentially irreversible component in the dissociation curves at 37°C is unknown, but may be involved in the mechanism by which IL-7 is able to transduce a biological signal at low receptor occupancy. Control experiments showed that this irreversibly bound ^{125}I-IL-7 was still on the cell surface even 90 min after initiation of dissociation since essentially all of it could be released by a low pH wash (data not shown). It is also apparent from these experiments that the initial rate of dissociation at 37°C is much more rapid than at 4°C, which supports conclusions reached from association kinetic experiments.

Specificity and Cellular Distribution of IL-7 Receptors. The specificity of murine IL-7 was assessed by testing a number of purified cytokines, as displayed in Table I, for their ability to compete with ^{125}I-IL-7 for binding to its receptor on IxN/2b cells.

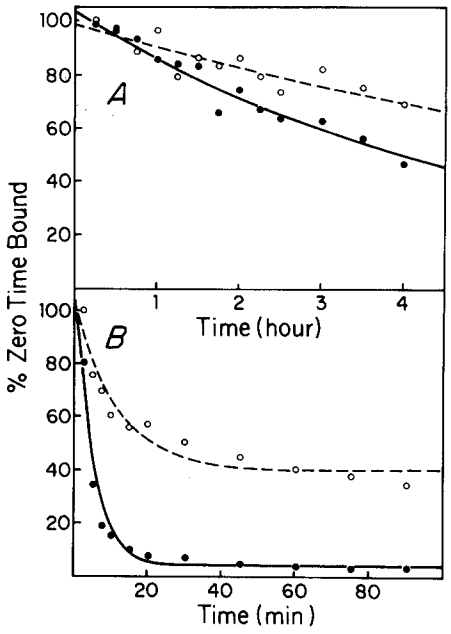

FIGURE 6. Dissociation kinetics of ^{125}I-IL-7 from IxN/2b cells. IxN/2b cells (1.33×10^7 cells/ml) were incubated with ^{125}I-IL-7 (4.0×10^{-10} M) for 2 h at 4°C. The cells were then split into two equal aliquots, harvested by centrifugation, and resuspended in either binding medium alone (○) or binding medium containing 8×10^{-8} M unlabeled IL-7 (●). The cells were maintained at either 4°C (*A*) or 37°C (*B*) and aliquots were removed at various times and assayed for binding as described under Materials and Methods. The concentration of ^{125}I-IL-7 present during dissociation was $<5.0 \times 10^{-12}$ M. Data obtained at 4°C (*A*) were analyzed with an exponential function that describes a simple first-order process. Dissociation rate constants calculated were: (○) $1.5 \pm 0.2 \times 10^{-3}$ min^{-1}; and (●) $3.1 \pm 0.2 \times 10^{-3}$ min^{-1}. Data obtained at 37°C (*B*) were analyzed with an equation that was the sum of an exponential function and a constant, which described the biphasic kinetic pattern consisting of a rapid initial dissociation rate followed by a slow component. Dissociation rate constants for the initial rapid rate were calculated to be: (○) $8.5 \pm 1.6 \times 10^{-2}$ min^{-1}; and (●) 0.20 ± 0.03 min^{-1}.

TABLE I
Specificity of ^{125}I-IL-7 Binding to IxN/2b Cells

Inhibitor	^{125}I-IL-7 bound*
	molecules/cell
None	380 ± 9
MuIL-7	45 ± 1
HuIL-1α	378 ± 9
HuIL-1β	384 ± 1
HuIL-2	389 ± 4
MuIL-4	396 ± 7
HuIL-5	379 ± 13
HuIL-6	385 ± 9
MuGM-CSF	400 ± 8
HuG-CSF	396 ± 15
HuCSF-1	384 ± 3
HuTGF-β	405 ± 8
HuTNF-α	400 ± 12
HuTNF-β	371 ± 25
MuINF-γ	382 ± 4
Hu Insulin	334 ± 2
Mu EGF	335 ± 11

IxN/2b cells were incubated for 30 min at 37°C with ^{125}I-IL-7 and unlabeled proteins as indicated at a 200-fold or greater molar excess. Binding was assayed as described under Materials and Methods.

When present in concentrations that were at a 200-fold or greater molar excess as compared with ^{125}I-IL-7, none of the other molecules exhibited any significant capacity to compete.

The cellular distribution of murine IL-7 receptors was also examined on a variety of primary cells and in vitro cell lines. As shown in Table II, IL-7 receptors were variably expressed on cells of both lymphoid and myelomonocytic origins. For all cell types shown in Table II, complete binding curves were done over a range of ^{125}I-IL-7 concentrations and receptor numbers per cell were generated by Scatchard analysis of the data. In all cases, ^{125}I-IL-7 binding generated curvilinear Scatchard plots, although the ratio of high to low affinity sites and the exact affinity constants obtained varied somewhat. Due to the fact that it is necessary to average several complete sets of binding data to obtain accurate binding constants from the high and low affinity portions of curvilinear Scatchard plots, we have reported only the total specific binding sites per cell in Table II. Not unexpectedly, all pre- and pro-B cell lines tested expressed significant levels of IL-7 receptors. In contrast, three B cell lines with a more mature phenotype as well as purified primary mature B cells did not express detectable levels of IL-7 receptor. Murine thymocytes, as well as a number of cell lines of the T cell lineage also expressed IL-7 receptors. Although most cell lines of myelomonocytic origin did not express detectable IL-7 receptors, quite surprisingly, bone marrow-derived macrophages, as well as the macrophage tumor line PU5-1.8, displayed significant levels of IL-7 receptor. In addition, the receptor was expressed on a variety of primary tissue sources including bone marrow, lymph node, and spleen at relatively low levels.

TABLE II
Distribution of Murine IL-7 Receptors

Designation	Characteristics	IL-7 bound*
		molecules/cell
Primary cells		
Bone marrow	BALB/c	360
BM macrophage	C3H	3,900
B cells	C57BL/6	<20
Lymph node cells	B10 and B6/C3H	860 ± 40
Spleen cells	CBA/N and B6	640 ± 20
Thymocytes	CBA/N and B6	330 ± 10
Cell lines		
IxN/2b	IL-7-dependent pre-B	2,510 ± 190
Abl 1.1	Pre-B	12,200
70Z/3	Pre-B lymphocyte	4,600
NFS-5 C-1	Pre-B lymphoblast	6,100
NFS-25 C-3	Pre-B lymphoblast	6,800
NFS-70 C-10	Pro-B lymphoblast	9,900
RAW 8.1	Early B lymphoma	1,900
ABE-8.1/2	Pre-B lymphoma	4,700
BCL-1	B cell lymphoma	<20
NS1	Myeloma	<20
8.653	Myeloma	<20
CTLL	Cytotoxic T cell	<20
HT-2	Helper T cell	<20
EL-4	T lymphoma	<20
YAC-1	T lymphoma	2,530
LBRM-33	T lymphoma	<20
LBRM-33-1A5	T lymphoma	3,400
LBRM-33-5A4	T lymphoma	1,600 ± 400
LSTRA	T-lymphocytic leukemia	1,100 ± 100
32D	Mast cell	<20
P815	Mastocytoma	<20
WEHI-3	Myelomonocytic	<20
FDCP-2	Myeloid	<20
$P388D_1$	Macrophage tumor	<20
J774	Macrophage tumor	<20
PU5-1.8	Macrophage tumor	8,300 ± 4,900

Binding experiments were conducted as described in the legend to Fig. 4. Molecules bound per cell were determined by Scatchard analysis of complete sets of binding data and represent total sites per cell. The limit of detection is defined as 20 molecules bound per cell.

Affinity Crosslinking. The molecular structure of the IL-7 receptor on IxN/2b cells was next examined by affinity crosslinking. Cells were incubated with radiolabeled IL-7 in the presence or absence of unlabeled IL-7, crosslinked with the water-soluble bifunctional reagent BS^3, and extracted with PBS/1% Triton containing a cocktail of protease inhibitors. The soluble fractions were then analyzed by SDS-PAGE under both reducing (Fig. 7, lanes *a–c*) and nonreducing (Fig. 7, lanes *d–f*) conditions. Two major crosslinked bands were observed under both conditions (Fig. 7, lanes *b* and *e*). Control experiments showed that no crosslinked species were found in the

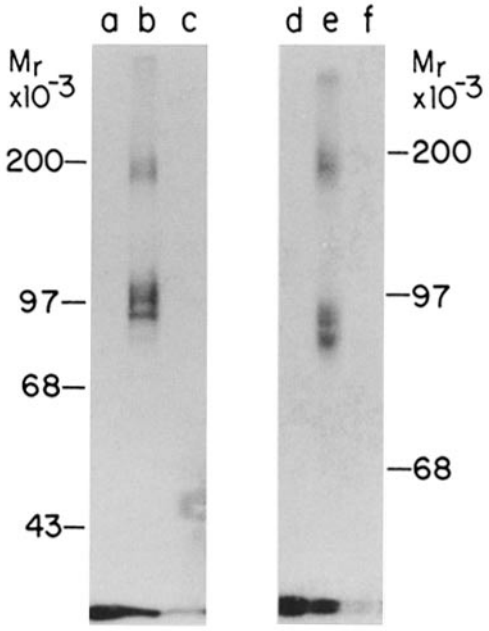

FIGURE 7. Characterization of IL-7 receptor by affinity crosslinking. IxN/2b cells (1.5×10^7) were incubated with ^{125}I-IL-7 (1×10^{-9} M) both in the absence (lanes *a*, *b*, *d*, *e*) and presence (lanes *c*, *f*) of unlabeled IL-7 (1×10^{-6} M). Incubation was for 2 h at 4°C and cells were then harvested, washed, crosslinked, and extracted as described under Materials and Methods. Lanes *a* and *d* depict control samples in which all procedures were conducted except for addition of crosslinker. Aliquots corresponding to 2×10^6 cells were boiled in sample buffer containing 2% SDS either with (lanes *a–c*) or without 5% 2-ME (lanes *d–f*) and subjected to electrophoresis on an 8% polyacrylamide gel. M_r values for crosslinked bands are determined by comparing R_f values to a standard curve generated by a linear least squares fit of the R_f values of the ^{14}C-standards.

absence of crosslinker (lanes *a* and *d*) or in samples containing excess unlabeled IL-7 (lanes *c* and *f*). From multiple crosslinking experiments the average relative molecular mass for the two species was calculated to be 186,300 ± 4,300 and 100,000 ± 1,300 under reducing conditions and 184,000 ± 2,100 and 103,500 ± 1,000 under nonreducing conditions. After subtraction of the molecular weight of IL-7 (25,000 M_r), the crosslinked species would correspond to membrane proteins of M_r 161,300 and 75,000 under reducing conditions and M_r 159,100 and 78,500 under nonreducing conditions. The diffuse nature of the crosslinked species and the appearance of two apparently distinct bands within the lower molecular weight band are likely due to variable levels of glycosylation on the receptor, IL-7 itself (see Fig. 2) or a combination of both. We cannot exclude the possibility, however, that these two bands represent crosslinking of IL-7 to nonidentical protein species. Interestingly, the larger receptor species has a molecular weight almost exactly twice that of the smaller receptor species, raising the possibility that it may represent a receptor dimer. It does not appear that the larger species is due to disulfide-linked subunits, since an almost identical crosslinking pattern is obtained under reducing and nonreducing conditions. In addition, control experiments in which crosslinked cells were extracted in PBS/1% Triton in the complete absence of any protease inhibitors revealed that the relative intensities of the two crosslinked bands were totally unchanged, suggesting that the lower molecular weight species is not a proteolytic degradation product of the larger species (data not shown). If the larger crosslinked species was due to the presence of receptor dimers, it was possible that the relative abundance of this species might be altered when crosslinking experiments were performed at varying IL-7 concentrations. We found, however, that the relative intensities of the high and low molecular weight species remained constant when crosslinking experiments were

performed with IL-7 concentrations ranging from 1×10^{-10} M to 3×10^{-9} M (data not shown). In addition, over this range, the calculated molecular weights of the crosslinked bands did not change, nor was there any appearance of higher molecular weight aggregates.

Discussion

We report here the isolation of an IL-7-dependent cell line, designated IxN/2b, which has been used as the basis for a consistent and sensitive bioassay for IL-7. The bioassay system originally used for the detection and isolation of murine IL-7 used freshly isolated B cell progenitors from long-term Whitlock-Witte bone marrow cultures. We now routinely use the IxN/2b cells as target cells in IL-7 bioassays. On a per-cell basis, the IxN/2b cell line incorporates approximately four times as much thymidine as pre-B cells grown in Whitlock-Witte bone marrow cultures. The cells are quite sensitive to stimulation with IL-7, and under the conditions of the assay they demonstrate a half-maximal stimulation response at ~0.05 ng/ml of IL-7, which translates to a half-maximal concentration of 3.3 pM.

Since the IxN/2b cell line is absolutely dependent on IL-7 for growth and viability, it also provided an ideal model in which to study putative cell surface receptors for IL-7. Although murine IL-7 contains only a single tyrosine residue very near the NH_2 terminus of the molecule, we found this residue could be almost quantitatively radiolabeled with ^{125}I to produce a homogeneous radiolabeled preparation that retained full biological activity in an IxN/2b proliferation assay. We determined that ^{125}I-IL-7 bound rapidly to IxN/2b cells at both 4° and 37°C, although the association rate was ~10 times faster at 37°C, reaching equilibrium within 15 min. Equilibrium binding studies revealed that ^{125}I-IL-7 binding produced curvilinear Scatchard plots at both temperatures, with a high affinity component having a K_a of $\sim 1 \times 10^{10}$ M^{-1} and a low affinity component with a K_a of $\sim 4 \times 10^8$ M^{-1}. Of the 2,000–2,500 total IL-7 binding sites expressed per cell, ~15–20% were of the high affinity type. Experiments designed to measure the affinity of unlabeled IL-7 by its ability to inhibit the binding of ^{125}I-IL-7 to its receptor also produced data consistent with the existence of two classes of IL-7 receptors on IxN/2b cells, with affinities similar to those obtained by direct ^{125}I-IL-7 binding.

Some evidence concerning the possible molecular nature of two classes of IL-7 receptors was provided by dissociation kinetics and affinity crosslinking experiments. There are several possible reasons for the appearance of curvilinear Scatchard plots including (*a*) the presence of two or more noninteracting binding sites with unchanging and dissimilar affinities; (*b*) the existence of multiple "affinity states" of a single receptor species, as a result, for instance, of variable phosphorylation or other modifications; and (*c*) the presence of negative cooperativity, such that the affinity of the overall receptor population decreases with increasing occupancy of receptors. Curvilinear Scatchard plots can also be caused artifactually by nonhomogeneous radiolabeled ligand preparations containing species displaying varying affinity or kinetic constants, or by the tendency of a ligand to aggregate at high concentrations to produce dimers or multimers possessing decreased receptor binding. A diagnostic test to distinguish between multiple noninteracting receptor species and receptor populations displaying negative cooperative behavior was first described by Demeyts et al. (32), in which

the dissociation rate of radiolabeled ligand is measured both in the presence and absence of an excess of unlabeled ligand. If negative cooperativity among the receptors exists, filling of receptors with unlabeled ligand may decrease the overall affinity of the receptor population and can potentially accelerate the rate of radioligand dissociation. When this experiment was performed with IxN/2b cells, we found that the dissociation rate of ^{125}I-IL-7 was markedly increased by the presence of unlabeled IL-7 at both 37° and 4°C. One possible explanation for this behavior is that the IL-7 receptor contains a binding subunit that can form noncovalently associated dimers in the membrane. Curvilinear Scatchard plots would be expected to result if the dimer species was capable of binding IL-7 with a higher affinity than the monomer. In addition, if the monomer and dimer species were present in an equilibrium that could be shifted towards the presence of low affinity monomers as the IL-7 concentration increased, apparent negative cooperative behavior could be observed. In its most strict definition, negative cooperativity refers to a system in which a continuous change in affinity of a receptor population is induced by ligand binding. Although the dissociation kinetics experiments can be operationally defined as exhibiting negative cooperative behavior, we do not yet have sufficient information to infer what molecular mechanisms are producing it.

Additional evidence that the IL-7 receptor may exist, at least partially, as a non-disulfide-linked dimer, was provided by affinity crosslinking experiments. Under both reducing and nonreducing conditions the major crosslinked species observed had a molecular mass of 100–104 kD, corresponding to a receptor size of 75–79 kD. In addition, a less intense higher molecular weight crosslinked species was also seen under both reducing and nonreducing conditions with a molecular mass of 184–187 kD, corresponding to a receptor size of 159–162 kD. The larger species therefore has a molecular mass slightly higher than twice that of the smaller species, suggesting that it may be a receptor dimer crosslinked to one (or possibly two) molecules of ^{125}I-IL-7. We cannot rule out at this point that the 184–187-kD form is due to crosslinking of ^{125}I-IL-7 to a receptor species distinct from that producing the 100–104-kD form, or even due to crosslinking of ^{125}I-IL-7 to a complex of the 75–79-kD protein plus an additional subunit. It appears unlikely, however, from experiments done in the presence and absence of protease inhibitors, that the smaller species is a proteolytic degradation product of the larger form.

In recent years, evidence for dimerization of receptor subunits has been reported for several growth factor receptor systems. The EGF receptor is perhaps the best example. Binding experiments with ^{125}I-EGF, which is a monomeric ligand, frequently generate curvilinear Scatchard plots (33). It has been shown that the EGF receptor can exist in both monomeric and dimeric states and that EGF binds to dimeric receptors with higher affinity than it does to monomeric receptors. Furthermore, the binding of EGF has been shown to induce receptor dimerization, which results in an increased tyrosine protein kinase activity compared with that observed for monomeric receptors (34–37). Recently, evidence has also been presented that high affinity binding of platelet-derived growth factor (PDGF), a dimeric ligand consisting of several isoforms, requires association of two different receptor subunits, and can in fact induce receptor dimerization (38–40). As with the EGF receptor, this dimerization has been correlated with an activation of the protein tyrosine kinase activity of the PDGF receptor (39). Even the insulin receptor, which consists

of a disulfide-linked $\alpha_2\beta_2$ heterotetramer, has been shown to bind ^{125}I-insulin with much lower affinity when dissociated into functional α/β heterodimers (41, 42).

While dissociation kinetics and affinity crosslinking experiments with ^{125}I-IL-7 suggest that the IL-7 receptor may exist in both monomeric and dimeric forms, we have no evidence that IL-7 itself is capable of inducing receptor dimerization. We have seen no evidence from gel filtration experiments that IL-7 has a propensity to form dimeric or oligomeric species in solution. In addition, crosslinking experiments done with varying concentrations of ^{125}I-IL-7 did not show an alteration in the amount of the higher molecular weight crosslinked species. A more definitive assessment of the role that receptor dimerization may play in generating the observed binding characteristics of the IL-7 receptor, and whether additional heterogeneity may also exist in the interaction of IL-7 with its receptor binding protein(s), will require further analysis.

In addition to characterization of the IL-7 receptor on the pre-B cell line IxN/2b, we also examined a variety of primary cells and in vitro cell lines for their ability to express IL-7 receptors. Although the levels of expression ranged from a few hundred to a few thousand receptors per cell, all cell types that were found to bind ^{125}I-IL-7 exhibited curvilinear Scatchard plots with high and low affinity binding constants in the same range as those calculated for IxN/2b cells. Not unexpectedly, all pre- and pro-B cell lines examined displayed relatively abundant levels of IL-7 receptors. However, three B cell lines of a more mature phenotype, as well as purified primary mature B cells failed to bind detectable levels of ^{125}I-IL-7. Although it is possible that mature B cells express IL-7 receptors at levels below the assay sensitivity, this receptor display correlates with the known biological activities of IL-7 on the B cell lineage, where no effects of IL-7 on mature B cells have yet been observed (3, 43). In addition, the IL-7 receptor was found to be expressed at low levels on murine thymocytes and on some, but not all, T lineage cell lines tested. Although IL-7 was originally isolated as a pre-B cell growth factor, it has subsequently been found to stimulate both T cell progenitors (5–7) and mature T cells as well (8, 9). Most surprisingly, IL-7 receptor was found to be expressed at relatively high levels on bone marrow–derived macrophages, as well as PU5-1.8, a macrophage tumor cell line. Although several other cell lines of myelomonocytic origin were negative, the presence of IL-7 receptors on two macrophage populations suggests that IL-7 may have as yet unexplored effects on cells outside the lymphoid compartment. This would not be totally unexpected given our prior observations regarding the effects of IL-7 on megakaryocyte differentiation (44).

Characterization of IL-7 receptors on different cell lineages, as well as further exploration into the role that dimerization of the IL-7 receptor may play in IL-7 signal transduction, should provide future insights into the mechanism and specificity of IL-7 action.

Summary

A murine cell line (IxN/2b) absolutely dependent upon exogenous IL-7 for continued growth has been obtained that expresses lymphoid precursor and class I MHC antigens and also contains a rearranged μ heavy chain. This cell line has been used to define the binding and structural characteristics of the murine IL-7 receptor using ^{125}I-labeled recombinant murine IL-7. ^{125}I-IL-7 binding to IxN/2b cell was rapid

and saturable at both 4° and 37°C. Equilibrium binding studies produced curvilinear Scatchard plots at both temperatures with high and low affinity K_a values of $\sim 1 \times 10^{10}$ M^{-1} and 4×10^8 M^{-1}, respectively, and a total of 2,000–2,500 IL-7 binding sites expressed per cell. Experiments measuring inhibition of binding of ^{125}I-IL-7 by unlabeled IL-7 also produced data consistent with the existence of two classes of IL-7 receptors. Evidence concerning the possible molecular nature of two classes of IL-7 receptors was provided by dissociation kinetics and affinity crosslinking experiments. The dissociation rate of ^{125}I-IL-7 was markedly increased when measured in the presence of unlabeled IL-7 at both 37° and 4°C, which is diagnostic of a receptor population displaying negative cooperativity. Crosslinking studies showed that under both reducing and nonreducing conditions, the major crosslinked species observed corresponded to a receptor size of 75–79 kD while a less intense higher molecular mass crosslinked species was also seen which corresponded to a receptor size approximately twice as large (159–162 kD). Both types of experiments suggest that the IL-7 receptor may form noncovalently associated dimers in the membrane. The IL-7 receptor was expressed on pre-B cells, but not detected on several mature B cell lines or primary mature B cells. It was also expressed on murine thymocytes, some T lineage cell lines, and on bone marrow–derived macrophage. All cells binding ^{125}I-IL-7 exhibited curvilinear Scatchard plots. No cytokines or growth factors tested were able to inhibit binding of ^{125}I-IL-7 to its receptor. These results define the initial binding and structural characteristics, and the cellular distribution, of the murine IL-7 receptor.

We thank Dr. Robert Tushinski for preparation of bone marrow macrophages, Drs. Kenneth Grabstein and William Fanslow for preparation of murine B cells, Deb Wood for binding analysis on many of the in vitro cell lines, and Alan Alpert for FACS analysis. We also thank Linda Troup for her help in preparation of this manuscript.

Received for publication 25 October 1989 and in revised form 21 December 1989.

References

1. Broxmeyer, H. E., and D. E. Williams. 1988. The production of myeloid blood cells and their regulation during health and disease. *CRC Crit. Rev. Hematol. Oncol.* 8:173.
2. Paul, W. E. 1989. Pleiotropy and redundancy: T cell-derived lymphokines in the immune response. *Cell.* 57:521.
3. Namen, A. E., A. E. Schmierer, C. J. March, R. W. Overell, L. S. Park, D. L. Urdal, and D. Y. Mochizuki. 1988. B cell precursor growth-promoting activity. Purification and characterization of a growth factor active on lymphocyte precursors. *J. Exp. Med.* 167:988.
4. Namen, A. E., S. Lupton, K. Hjerrild, J. Wignall, D. Y. Mochizuki, A. Schmierer, B. Mosley, C. J. March, D. Urdal, S. Gillis, D. Cosman, and R. G. Goodwin. 1988. Stimulation of B-cell progenitors by cloned interleukin-7. *Nature (Lond.).* 333:571.
5. Conlon, P. J., P. J. Morrissey, R. P. Nordan, K. H. Grabstein, K. S. Prickett, S. G. Reed, R. Goodwin, D. Cosman, and A. E. Namen. 1989. Murine thymocytes proliferate in direct response to interleukin-7. *Blood.* 74:1368.
6. Chantry, D. M., M. Turner, and M. Feldman. 1989. Interleukin 7 (murine pre-B cell growth factor/lymphopoietin 1) stimulates thymocyte growth: regulation by transforming growth factor beta. *Eur. J. Immunol.* 19:783.
7. Watson, J. D., P. J. Morrissey, A. E. Namen, P. J. Conlon, and M. B. Widmer. 1989. Effect of IL-7 on the growth of fetal thymocytes in culture. *J. Immunol.* 143:1215.

8. Morrissey, P. J., R. G. Goodwin, R. P. Nordan, D. Anderson, K. H. Grabstein, D. Cosman, J. Sims, S. Lupton, B. Acres, S. G. Reed, D. Y. Mochizuki, J. Eisenman, P. J. Conlon, and A. E. Namen. 1989. Recombinant interleukin 7, pre-B cell growth factor, has costimulatory activity on purified mature T cells. *J. Exp. Med.* 169:707.
9. Chazen, G. D., G. M. B. Pereira, G. Legros, S. Gillis, and E. M. Shevach. 1989. Interleukin 7 is a T-cell growth factor. *Proc. Natl. Acad. Sci. USA.* 86:5923.
10. Grabstein, K. H., A. E. Namen, K. Shanebeck, R. F. Voice, S. G. Reed, and M. B. Widmer. 1990. Regulation of T cell proliferation by interleukin-7. *J. Immunol.* In press.
11. Rosenberg, N., and D. Baltimore. 1976. A quantitative assay for transformation of bone marrow cells by Abelson murine leukemia virus. *J. Exp. Med.* 49:355.
12. Grabstein, K. H., L. S. Park, P. J. Morrissey, H. Sassenfeld, V. Price, D. L. Urdal, and M. B. Widmer. 1987. Regulation of murine T cell proliferation by B cell stimulatory factor-1. *J. Immunol.* 139:1148.
13. Tushinski, R. J., I. T. Oliver, L. J. Guilbert, P. W. Tynan, J. R. Warner, and E. R. Stanley. 1982. Survival of mononuclear phagocytes depends on lineage-specific growth factor that the differentiated cells selectively destroy. *Cell.* 28:71.
14. Kronheim, S. R., M. A. Cantrell, M. C. Deeley, C. J. March, P. J. Glackin, D. A. Anderson, T. Hemenway, J. E. Merriam, D. Cosman, and T. P. Hopp. 1986. Purification and characterization of human interleukin-1 expressed in *Escherichia coli*. *Biotechnology.* 4:1078.
15. Price, V., D. Mochizuki, C. J. March, D. Cosman, M. C. Deeley, R. Klinke, W. Clevenger, S. Gillis, P. Baker, and D. Urdal. 1987. Expression, purification and characterization of recombinant murine granulocyte-macrophage colony-stimulating factor and bovine interleukin-2 from yeast. *Gene (Amst.).* 55:287.
16. Park, L. S., D. Friend, K. Grabstein, and D. L. Urdal. 1987. Characterization of the high affinity cell-surface receptor for murine B-cell stimulating factor 1. *Proc. Natl. Acad. Sci. USA.* 84:1669.
17. Hopp, T. P., K. S. Prickett, V. L. Price, R. T. Libby, C. J. March, D. P. Cerretti, D. L. Urdal, P. J. Conlon. 1988. A short polypeptide marker sequence useful for recombinant protein identification and purification. *Biotechnology.* 6:1204.
18. Park, L. S., P. E. Waldron, D. Friend, H. M. Sassenfeld, V. Price, D. Anderson, D. Cosman, R. G. Andrews, I. D. Bernstein, and D. L. Urdal. 1989. Interleukin-3, GM-CSF, and G-CSF receptor expression on cell lines and primary leukemia cells: receptor heterogeneity and relationship to growth factor responsiveness. *Blood.* 74:56.
19. Dennert, G., R. Hyman, J. Lesley, and I. S. Trowbridge. 1980. Effect of cytotoxic monoclonal antibody specific for T200 glycoprotein on functional lymphoid cell populations. *Cell. Immunol.* 53:350.
20. Ledbetter, J. A., and L. A. Herzenberg. 1979. Xenogeneic monoclonal antibodies to mouse lymphoid differentiation antigens. *Immunol. Rev.* 47:63.
21. Bruce, J., F. W. Symington, T. J. McKearn, and J. Sprent. 1981. A monoclonal antibody discriminating between subsets of T and B cells. *J. Immunol.* 127:2496.
22. Malek, T. R., R. J. Robb, and E. M. Shevach. 1983. Identification and initial characterization of a rat monoclonal antibody reactive with the murine interleukin 2 receptor-ligand complex. *Proc. Natl. Acad. Sci. USA.* 80:5694.
23. Koo, G. C., and J. R. Peppard. 1984. Establishment of monoclonal anti-NK1.1 antibody. *Hybridoma.* 3:301.
24. Lesley, J., R. Schulte, J. Trotter, and R. Hyman. 1988. Qualitative and quantitative heterogeneity in Pgp-1 expression among murine thymocytes. *Cell. Immunol.* 112:40.
25. Kincade, P. W., G. Lee, T. Watanabe, L. Sun, and M. P. Scheid. 1981. Antigens displayed on murine B lymphocyte precursors. *J. Immunol.* 127:262.
26. Ho, M., and T. A. Springer. 1982. Mac-1 antigen: Quantitative expression in macro-

phage populations and tissues and immunofluorescent localization in the spleen. *J. Immunol.* 128:2281.

27. Park, L. S., D. Friend, S. Gillis, and D. L. Urdal. 1986. Characterization of the cell surface receptor for granulocyte-macrophage colony-stimulating factor. *J. Biol. Chem.* 261:4177.
28. Dower, S. K., K. Ozato, and D. M. Segal. 1984. The interaction of monoclonal antibodies with MHC class I antigens on mouse spleen cells. Analysis of the mechanism of binding. *J. Immunol.* 132:751.
29. Dower, S. K., J. A. Titus, C. DeLisi, and D. M. Segal. 1981. Mechanism of binding of multivalent immune complexes to Fc Receptors. 2. Kinetics of binding. *Biochemistry.* 20:6335.
30. Dower, S. K., C. DeLisi, J. A. Titus, and D. M. Segal. 1981. Mechanism of binding of multivalent immune complexes to Fc receptors. I. Equilibrium binding. *Biochemistry.* 20:6326.
31. Laemmli, U. K. 1970. Cleavage of structural proteins during the assembly of the head of bacteriophage T4. *Nature (Lond.).* 227:680.
32. Demeyts, P., J. Roth, D. M. Neville, J. R. Gavin, and M. Lesniak. 1973. Insulin interactions with its receptors: experimental evidence for negative cooperativity. *Biochem. Biophys. Res. Commun.* 55:154.
33. Schlessinger, J. 1988. The epidermal growth factor receptor as a multifunctional allosteric protein. *Biochemistry.* 27:3119.
34. Yarden, Y., and J. Schlessinger. 1987. Self-phosphorylation of epidermal growth factor receptor: evidence for a model of intermolecular allosteric activation. *Biochemistry.* 26:1434.
35. Yarden, Y., and J. Schlessinger. 1987. Epidermal growth factor induces rapid, reversible aggregation of the purified epidermal growth factor receptor. *Biochemistry.* 26:1443.
36. Boni-Schnetzler, M., and P. F. Pilch. 1987. Mechanism of epidermal growth factor receptor autophosphorylation and high-affinity binding. *Proc. Natl. Acad. Sci. USA.* 84:7832.
37. Cochet, C., O. Kashles, E. M. Chambaz, I. Borrello, C. R. King, and J. Schlessinger. 1988. Demonstration of epidermal growth factor-induced receptor dimerization in living cells using a chemical covalent cross-linking agent. *J. Biol. Chem.* 263:3290.
38. Seifert, R. A., C. E. Hart, P. E. Phillips, J. W. Forstrom, R. Ross, M. J. Murray, and D. F. Bowen-Pope. 1989. Two different subunits associate to create isoform-specific platelet-derived growth factor receptors. *J. Biol. Chem.* 264:8771.
39. Heldin, C.-H., A. Ernlund, C. Rorsman, and L. Ronnstrand. 1989. Dimerization of B-type platelet-derived growth factor receptors occurs after ligand binding and is closely associated with receptor kinase activation. *J. Biol. Chem.* 264:8905.
40. Hammacher, A., K. Mellstrom, C.-H. Heldin, and B. Westermark. 1989. Isoform-specific induction of actin reorganization by platelet-derived growth factor suggests that the functionally active receptor is a dimer. *EMBO (Eur. Mol. Biol. Organ.) J.* 8:2489.
41. Sweet, L. J., B. D. Morrisson, and J. E. Pessin. 1987. Isolation of functional $\alpha\beta$ heterodimers from the purified human placental $\alpha_2\beta_2$ heterotetrameric insulin receptor complex. *J. Biol. Chem.* 262:6939.
42. Boni-Schnetzler, M., W. Scott, S. M. Waugh, E. DiBella, and P. F. Pilch. 1987. The insulin receptor. Structural basis for high affinity ligand binding. 1987. *J. Biol. Chem.* 262:8395.
43. Lee, G., A. E. Namen, S. Gillis, L. R. Ellingsworth, and P. W. Kincade. 1989. Normal B cell precursors responsive to recombinant murine IL-7 and inhibition of IL-7 activity by transforming growth factor-β. *J. Immunol.* 142:3875.
44. Williams, D. E., D. Krumwieh, F. Seiler, D. L. Urdal, S. Gillis, and A. E. Namen. 1990. Cytokine effects on megakaryocytopoiesis. *UCLA (Univ. Calif. Los Angel.) Symp. Mol. Cell. Biol.* In press.